178 *Organometallics* **2004,** *23,* 178−183

Articles

Syntheses and Crystal Structures of Simple Dibenzylcalcium Complexes: Useful Reagents in the Preparation of Calcium Compounds

Sjoerd Harder,* Stefanie Müller, and Eike Hübner

Universität Konstanz, Postfach 5560-M738, 78457 Konstanz, Germany

Received August 27, 2003

Synthetic routes to dibenzylcalcium or *para*-substituted dibenzylcalcium complexes are described. Crystal structures of *trans*-(*p*-*t*Bu-benzyl)$_2$Ca·(THF)$_4$ and *cis*-(benzyl)$_2$Ca·(THF)$_4$ show similar Ca−C and Ca−O bond distances. The observation of different geometries (*cis*/*trans*) is explained by packing effects (DFT methods calculate less than 2 kcal/mol energy difference between *cis*- and *trans*-geometries). The strongly basic dibenzylcalcium complexes are useful precursors in calcium chemistry. Triphenylmethane was deprotonated, and the highly symmetric structure of [Ph$_3$C$^-$]$_2$[Ca^{2+}·(THF)$_6$] is discussed.

Introduction

The organometallic chemistry of the heavier alkaline-earth metals (Ca, Sr, and Ba) is developing fast; however, information on the more reactive σ-bonded alkyl or benzyl complexes is still scarce.[1] We recently published synthetic routes and crystal structures for two dibenzylcalcium complexes (**1** and **2**).[2,3]

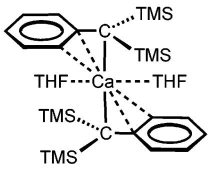

1

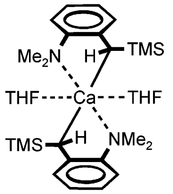

2

Both dibenzylcalcium complexes were obtained in good yields via a ligand metathesis reaction in THF (eq 1). The carbanions in **1** are stabilized by two Me$_3$Si substituents attached to the benzylic carbon. Complex **2** is stabilized by one Me$_3$Si substituent and an *ortho*-Me$_2$N substituent functioning as an intramolecular chelate arm. The Me$_3$Si substituents in **1** and **2** greatly reduce their reactivities, thus facilitating syntheses and handling. These bulky groups also prevent aggregation of the calcium complex and function as solubilizers, which allow the separation of the product from the precipitated KI (the Me$_2$N substituent in **2** has a similar function).

$$2\,\mathrm{RK} + \mathrm{CaI_2} \xrightarrow{\mathrm{THF}} \mathrm{R_2Ca} + 2\,\mathrm{KI}\downarrow \qquad (1)$$

The initial idea that the ligand metathesis route to dibenzylcalcium compounds needs stabilizing and solubilizing substituents such as the Me$_3$Si and Me$_2$N groups is now abandoned with the herein described successful syntheses of simple benzylcalcium complexes: bis(*para*-*tert*-butylbenzyl)calcium ((*p*-*t*BuBz)$_2$Ca), bis(*para*-trimethylsilylbenzyl)calcium ((*p*-Me$_3$SiBz)$_2$Ca), and dibenzylcalcium ((Bz)$_2$Ca). In addition, the crystal structures of (*p*-*t*BuBz)$_2$Ca·(THF)$_4$ and (Bz)$_2$Ca·(THF)$_4$ are compared. The potential of these compounds as highly reactive reagents in the synthesis of organocalcium complexes is shown by the successful deprotonation of Ph$_3$CH and HN(SiMe$_3$)$_2$. The crystal structure of one of the products, the solvent-separated ion-pair [Ph$_3$C$^-$]$_2$[Ca^{2+}·(THF)$_6$], is described with the “metal-in-a-box” model.[4]

Results and Discussion

The standard procedure for the preparation of dibenzylcalcium compounds is as follows: (i) reaction of 2 equiv of the benzylpotassium compound with CaI$_2$ in THF, (ii) evaporation of the solvent and extraction with benzene, (iii) crystallization from either hexane/THF or benzene/THF mixtures. Since step (ii) requires a soluble dibenzylcalcium product, substitution of the dibenzylcalcium compound in the *para*-position with either a *t*Bu or Me$_3$Si group seemed particularly advantageous. It was found, however, that even the unsubstituted dibenzylcalcium complex is well-soluble in aromatic solvents. All compounds were isolated as crystalline-pure etherate complexes of general formula Bz$_2$Ca·(THF)$_4$, which explains their excellent solubility in aromatic solvents.

Di(*p*-*tert*-butylbenzyl)calcium·(THF)$_4$ crystallizes as a monomer with a slightly distorted octahedral coordina-

---

* Corresponding author. E-mail: harder@chemie.uni-konstanz.de.

(1) (a) Hanusa, T. P. *Coord. Chem. Rev.* **2000**, *210*, 329. (b) Westerhausen, M. *Angew. Chem.* **2001**, *113*, 3063; *Angew. Chem., Int. Ed.* **2001**, *40*, 2975. (c) Alexander, J. S.; Ruhlandt-Senge; K. *Eur. J. Inorg. Chem.* **2002**, 2761.

(2) Feil, F.; Harder, S. *Organometallics* **2000**, *19*, 5010.

(3) Harder, S.; Feil, F.; Weeber, A. *Organometallics* **2001**, *20*, 1044.

(4) Harder, S.; Feil. F.; Repo, T. *Chem. Eur. J.* **2002**, *8*, 1991.

10.1021/om0341350 CCC: $27.50

Table 1. Selected Bond Distances (Å) and Angles (deg) for $(p\text{-}t\text{BuBz})_2\text{Ca}\cdot(\text{THF})_4$ and $(\text{Bz})_2\text{Ca}\cdot(\text{THF})_4$

$(p\text{-}t\text{BuBz})_2\text{Ca}\cdot(\text{THF})_4$		$(\text{Bz})_2\text{Ca}\cdot(\text{THF})_4$, molecule 1		$(\text{Bz})_2\text{Ca}\cdot(\text{THF})_4$, molecule 2	
Ca−C1	2.602(3)	Ca1−C1	2.595(5)	Ca2−C31	2.574(6)
Ca−C12	2.592(3)	Ca1−C8	2.587(6)	Ca2−C38	2.568(5)
Ca−O1	2.379(2)	Ca1−O1	2.376(3)	Ca2−O5	2.392(3)
Ca−O2	2.388(2)	Ca1−O2	2.400(3)	Ca2−O6	2.391(3)
Ca−O3	2.383(2)	Ca1−O3	2.446(3)	Ca2−O7	2.407(3)
Ca−O4	2.403(2)	Ca1−O4	2.389(3)	Ca2−O8	2.381(3)
C1−C2	1.433(4)	C1−C2	1.436(7)	C31−C32	1.411(8)
C12−C13	1.431(4)	C8−C9	1.425(8)	C38−C39	1.426(7)
O1−Ca−O2	99.13(7)	O1−Ca1−O3	82.5(1)	O5−Ca2−O6	84.2(1)
O1−Ca−O4	89.50(7)	O1−Ca1−O4	89.2(1)	O5−Ca2−O7	82.5(1)
O2−Ca−O3	86.29(7)	O2−Ca1−O3	85.6(1)	O5−Ca2−O8	88.1(1)
O3−Ca−O4	85.14(7)	O2−Ca1−O4	84.0(1)	O6−Ca2−O7	83.8(1)
C1−Ca−C12	176.37(9)	O3−Ca1−O4	80.1(1)	O7−Ca2−O8	84.1(1)
C2−C1−Ca1	118.5(2)	C1−Ca1−C8	97.2(2)	C31−Ca2−C38	90.9(2)
C13−C12−Ca1	118.1(2)	C2−C1−Ca1	117.7(3)	C32−C31−Ca2	124.4(4)
		C9−C8−Ca1	120.7(4)	C39−C38−Ca2	119.7(3)

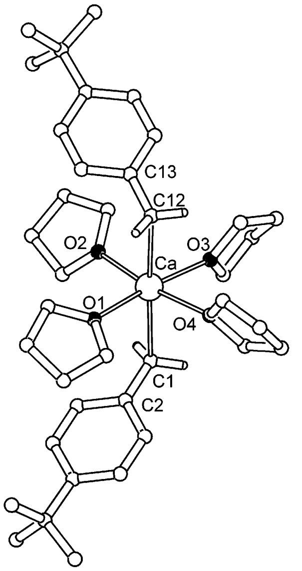

Figure 1. Crystal structure of $(p\text{-}t\text{BuBz})_2\text{Ca}\cdot(\text{THF})_4$. Only benzylic hydrogens are shown.

tion geometry around the calcium (Figure 1; selected bond distances and angles are summarized in Table 1). The benzyl carbanions are positioned *trans* with a nearly linear angle (C1−Ca−C12 = 176.37(9)°). Also the dibenzylcalcium compounds **1** and **2** display coordination geometries in which the carbanions are in *trans* position. This is likely due to electrostatic repulsion between the negatively charged benzylic carbons. All THF oxygens are situated in a plane; however, the O−Ca−O angles show a large variation (85.14(7)−99.13(7)°). Steric interactions between the phenyl rings and the THF ligands considerably widen the O1−Ca−O2 angle to 99.13(7)°, consequently squeezing other O−Ca−O valence angles. The Ca−C bond distances of 2.592(3) and 2.602(3) Å are very similar and slightly shorter than those observed in **1** (average 2.628(3) Å) or than those in **2** (2.649(2) Å). The C−C−Ca angles of 118.5(2)° and 118.1(2)° are slightly larger than a tetrahedral angle. The hybridization of the benzylic carbon is between sp^2 and sp^3: the sums of C−C−H and H−C−H angles are 342(2)° and 344(2)°.

Dibenzylcalcium·(THF)$_4$ likewise crystallizes as a monomer with a slightly distorted octahedral coordination geometry around the calcium. Figure 2 shows the two similar but crystallographically independent molecules within the asymmetric unit; selected bond distances and angles are summarized in Table 1. Surprisingly, both molecules show benzyl carbanions in *cis*-positions with angles C1−Ca1−C8 = 97.2(2)° and C31−Ca1−C38 = 90.9(2)°. The Ca−C and Ca−O distances in $(\text{Bz})_2\text{Ca}\cdot(\text{THF})_4$ are very much comparable to those observed in $(p\text{-}t\text{BuBz})_2\text{Ca}\cdot(\text{THF})_4$. Also the hybridization of the benzylic carbon is in a similar range: the average value for the sums of the valence angles at the benzylic carbons is 345(3)°.

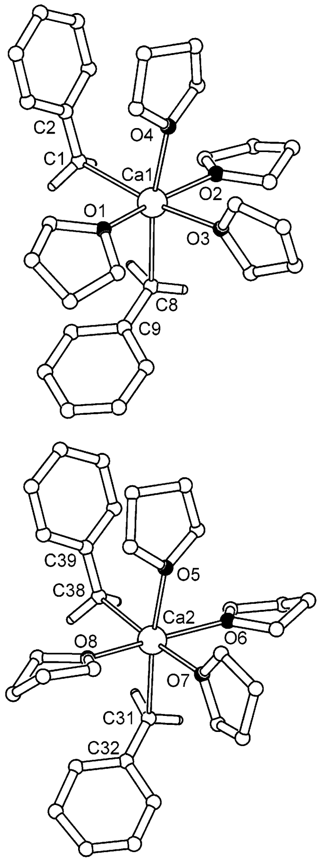

Figure 2. Two similar but crystallographically independent molecules are observed in the crystal structure of $(\text{Bz})_2\text{Ca}\cdot(\text{THF})_4$. Only benzylic hydrogens are shown.

The similarities in bond lengths for $(\text{Bz})_2\text{Ca}\cdot(\text{THF})_4$ and $(p\text{-}t\text{BuBz})_2\text{Ca}\cdot(\text{THF})_4$ contrast sharply with the differences observed in their coordination geometries (*cis*/*trans*) and poses the question why one compound

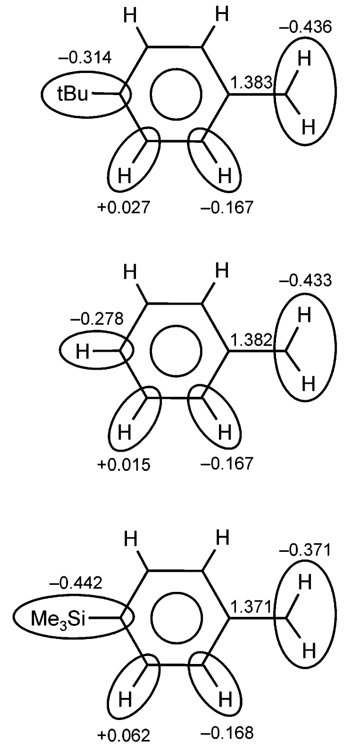

Figure 3. Ab initio (MP2/6-31+G*) group charges calculated with the NPA method and $C_\alpha-C_{ipso}$ bond lengths (Å) for the following benzyl anions: *p*-*t*BuBz$^-$, Bz$^-$, and *p*-Me$_3$SiBz$^-$ (all with C_s symmetry).

crystallizes in *cis*- and the other in *trans*-geometry. The *trans*-conformer maximizes the separation between the most negatively charged ligands, the benzyl ligands, and should be the more stable one. Differences in geometry might therefore be explained by the effect of the *para*-substituent on the charge at the benzylic carbon. The electron-releasing *t*Bu-substituent in (*p*-*t*BuBz)$_2$Ca·(THF)$_4$ could decrease the extent of benzylic charge delocalization. This would result in a higher electron density on the benzylic carbon and thus a stronger preference for a *trans*-geometry than in (Bz)$_2$Ca·(THF)$_4$. On the other hand, a Me$_3$Si substituent stabilizes negative charge in α-position, thus increasing charge delocalization. This would lead to less electron density on the benzylic carbon.

We calculated the effect of the *para*-substituent on the charge distribution in benzyl anions (Figure 3). In contrast to our expectations, a *t*Bu substituent in the *para*-position has a negligible effect on the electron density at the CH$_2$ group. This is also shown by the very similar $C_\alpha-C_{ipso}$ bond distances in *p*-*t*BuBz$^-$ and Bz$^-$. On the other hand, *para*-substitution of the benzyl anion with a Me$_3$Si group results in increased charge delocalization, as expected.

The influences calculated for *para*-substitution were confirmed by experiment. First of all, the $C_\alpha-C_{ipso}$ bond distances in the crystal structures of (*p*-*t*BuBz)$_2$Ca·(THF)$_4$ and (Bz)$_2$Ca·(THF)$_4$ are very similar: 1.433(4) and 1.424(8) Å, respectively. Also the ^1J(C−H) coupling constants for the benzylic C_α in (*p*-*t*BuBz)$_2$Ca·(THF)$_4$ and (Bz)$_2$Ca·(THF)$_4$ are very similar: 125.5 and 125.0 Hz, respectively. This is indicative of a similar hybridization at the benzylic carbon and thus of similar charge delocalization. The similar hybridization at the benzylic carbon is also confirmed by the geometries around the benzylic carbon (H atoms have been located) as observed in the crystal structures (vide infra).

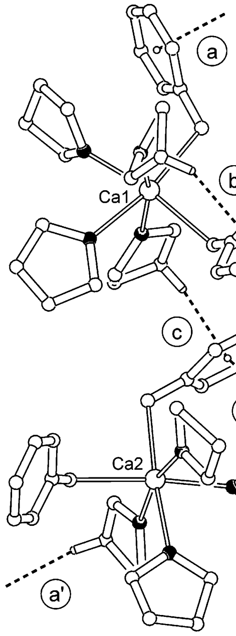

Figure 4. Network of C−H···π interactions in the crystal structure of (Bz)$_2$Ca·(THF)$_4$; only the hydrogens involved are shown. The following short H···aryl$_{center}$ contacts are observed (C−H···aryl$_{center}$ angles are given in parentheses): $a = 2.484$ Å (155.4°), $b = 2.712$ Å (147.4°), $c = 2.524$ Å (152.5°), and $d = 2.622$ Å (148.5°).

Although the crystal strucure of (*p*-Me$_3$SiBz)$_2$Ca·(THF)$_4$ could not be determined, experimental information on the extent of charge delocalization was obtained by measurement of the ^1J(C−H) coupling constant for the benzylic C_α. The value of 129.0 Hz indicates more sp^2 character and consequently more charge delocalization than in (*p*-*t*BuBz)$_2$Ca·(THF)$_4$ and (Bz)$_2$Ca·(THF)$_4$. This is in agreement with the calculated charge distributions (Figure 3).

The similarities in the charge distributions for (*p*-*t*BuBz)$_2$Ca·(THF)$_4$ and (Bz)$_2$Ca·(THF)$_4$ eliminate electronic effects as an explanation for their different geometries in the solid state. It also seems to be highly unlikely that steric effects influence the geometries of these *para*-substituted systems. Therefore, the *cis*- and *trans*-geometries of (*p*-*t*BuBz)$_2$Ca·(THF)$_4$, (Bz)$_2$Ca·(THF)$_4$, and (*p*-Me$_3$SiBz)$_2$Ca·(THF)$_4$ were investigated by DFT calculation. The *trans*-geometry is most stable in all cases; however, the differences in energy with the *cis*-geometry are extremely small (1.77, 1.97, and 1.71 kcal/mol, respectively). It is thus likely that the differences in geometries are caused by packing effects in the crystal. Short inter- and intramolecular distances indeed indicate a network of C−H···π interactions in the crystal structure of (Bz)$_2$Ca·(THF)$_4$ (Figure 4). The energy involved with such interactions[5] could balance the energy loss for a *cis*-geometry. The crystal structure of (*p*-*t*BuBz)$_2$Ca·(THF)$_4$ shows only one rather long intramolecular C−H···π interaction (H···aryl$_{center}$ = 2.758 Å and C−H···aryl$_{center}$ = 151.9°).

---

[5] Harder, S. *Chem. Eur. J.* **1999**, *5*, 1853.

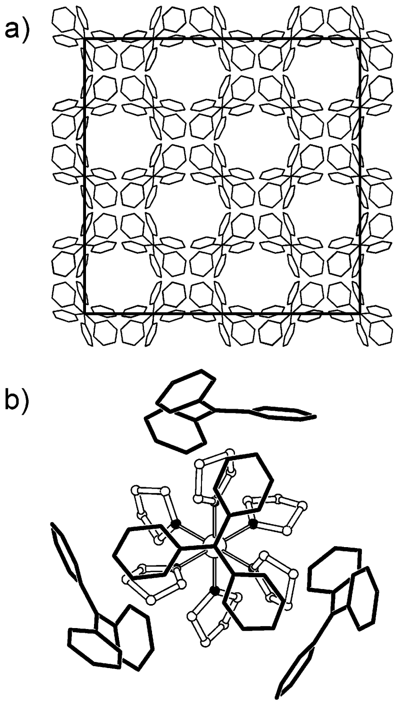

Figure 5. Crystal structure of $[Ph_3C^-]_2[Ca^{2+}\cdot(THF)_6]$: (a) packing of the 32 Ph_3C^- ions in the unit cell; (b) the $Ca^{2+}\cdot(THF)_6$ ion is embedded in a cavity spanned by four Ph_3C^- ions (hydrogens omitted for clarity).

The highly basic dibenzylcalcium compounds (pK_a of toluene: 43) presented here are potent deprotonating reagents or nucleophiles and can therefore be used in the syntheses of a variety of organocalcium compounds. The synthetic use of dibenzyl complexes of the heavier alkaline-earth metals has been demonstrated earlier for the dibenzylbarium reagent.[6,7] Reaction of $(Bz)_2Ca\cdot(THF)_4$ with 2 equiv of Ph_3CH in refluxing THF results in quantitative formation of $(Ph_3C)_2Ca\cdot(THF)_2$ in the form of a dark red powder. This compound is well-soluble in benzene, but can be fully precipitated by slow addition (vapor diffusion) of THF. This unusual solution behavior—polar solvents usually enhance the solubility of polar organometallic compounds—has been observed before[4] and is due to the formation of solvent-separated ion-pairs (here: $[Ph_3C^-]_2[Ca^{2+}\cdot(THF)_6]$).

These ion-pairs crystallize in a salt-like lattice of high cubic symmetry: spacegroup F_d-3.[8] Whereas the asymmetric unit contains only 1/3 of a Ph_3C^- ion and 1/6 of a $Ca^{2+}\cdot(THF)_6$ ion, the whole unit cell contains 32 Ph_3C^- ions and 16 $Ca^{2+}\cdot(THF)_6$ ions (there are 96 symmetry-equivalent positions). The propeller-like Ph_3C^- ions are positioned over 3-fold axes and are packed such that perpendicular channels are formed along the unit cell axes (Figure 4a). The $Ca^{2+}\cdot(THF)_6$ ions are located in these channels and are also positioned over 3-fold axes. This results in a unit with perfect tetrahedral symmetry (T_d) consisting of a $Ca^{2+}\cdot(THF)_6$ ion (all O−Ca−O angles are 90° or 180° due to symmetry) tetrahedrally surrounded by four Ph_3C^- ions (Figure 4b). The packing can be described with the "metal-in-a-box" model previously reported for other solvent-separated ion-pairs of the alkaline-earth metals.[4] The contact of the solvated cation with the walls of the pyramide-shaped box inevitably proceeds via the THF ligands. The shortest contact between anions and cations is that of a β-CH_2 proton of THF with the aryl ring of Ph_3C^-: $H\cdots aryl_{center}$ is 2.726 Å with an $C-H\cdots aryl_{center}$ angle of 136.5°.

Complex $(p\text{-}t\text{BuBz})_2Ca\cdot(THF)_4$ loses its THF ligands upon heating crushed crystals under vacuum (0.1 Torr, 60 °C, 1 h), and a THF-free dibenzylcalcium complex is obtained. This is remarkable since in general THF ligands are very hard to remove from organocalcium complexes.[9] The THF ligands in **1** and **2** could not be removed by heating under vacuum. The availability of a THF-free highly basic dibenzylcalcium compound also opens a route to the syntheses of THF-free calcium complexes; for example, reaction of $(p\text{-}t\text{BuBz})_2Ca$ with $HN(SiMe_3)_2$ in refluxing benzene results in complete conversion to the earlier reported THF-free $Ca[N(SiMe_3)_2]_2$[10] and avoids the use of toxic Sn compounds.

Conclusion

Simple benzylcalcium complexes $(p\text{-}t\text{BuBz})_2Ca$, $(p\text{-}Me_3SiBz)_2Ca$, and $(Bz)_2Ca$ can be prepared in crystalline form with reasonable yields (40−60%). The good solubility of these complexes can be explained by the presence of four THF ligands per Ca, which results in an octahedral coordination geometry at Ca. The energy differences between *cis*- and *trans*-geometries are very small (<2 kcal/mol), and crystal-packing effects are likely responsible for the different geometries in *trans*-$(p\text{-}t\text{BuBz})_2Ca\cdot(THF)_4$ and *cis*-$(Bz)_2Ca\cdot(THF)_4$ observed in the solid state.

These simple benzylcalcium complexes are potent deprotonating reagents. The complex $(p\text{-}t\text{BuBz})_2Ca\cdot(THF)_4$ can be freed of its THF ligands and could be a useful precursor in the syntheses of THF-free calcium complexes.

Experimental Section

General Comments. All experiments were carried out under argon using predried solvents and Schlenk techniques. Larger amounts of benzylpotassium were kindly provided by MCAT (Konstanz, Germany). Crystal diffraction data were measured on an Enraf-Nonius CAD4 diffractometer (crystal data are given in Table 2). Crystal structures were solved with DIRDIF[11] and refined with SHELXL-97.[12] Geometry calculations and graphics were done with PLATON.[13] In all structures the benzylic hydrogen atoms were observed and refined isotropically. Calculated hydrogen positions (C−H 1.08 Å) were

---

(6) Weeber, A.; Harder, S.; Brintzinger, H.-H.; Knoll, K. *Organometallics* **2000**, *19*, 1325.

(7) Alexander, J. S.; Ruhlandt-Senge, K. *Angew. Chem.* **2001**, *113*, 2732; *Angew. Chem., Int. Ed.* **2001**, *40*, 2658.

(8) Only 32 compounds out of ca. 250 000 entries were found in the Cambridge Crystallographic Database; this is 0.01% of all structures. Note that the structure of the isomorph $[Ph_3C^-]_2[Yb^{II}\cdot(THF)_6]$ has been solved faultily in the lower symmetry space group *Im*-3 with a 1/1 disorder in the Ph_3C^- ions (this could be due to twinning): Bochkarev, L. N.; Molosnova, N. E.; Zakharov, L. N.; Fukin, G. K.; Yanovsky, A. I., Struchkov, Y. T. *J. Organomet. Chem.* **1995**, *485*, 101.

(9) Andersen, R. A., Blom, R., Boncella, J. M.; Burns, C. J.; Volden, H. V. *Acta Chem. Scand. Ser. A* **1987**, *41*, 24.

(10) Westerhausen, M.; Schwarz, W. *Z. Anorg. Allg. Chem.* **1991**, *604*, 127.

(11) Beurskens, P. T.; Admiraal, G.; Beurskens, G.; Bosman, W. P.; de Gelder, R.; Israel, R. *The DIRDIF Program System;* Crystallography Laboratory, University of Nijmegen: The Netherlands, 1994.

(12) Sheldrick, G. M *SHELXL-97, Programs for the Determination of Crystal Structures*; Universität Göttingen: Germany, 1997.

(13) Spek, A. L. *PLATON, A Multipurpose Crystallographic Tool*; Utrecht University: Utrecht, The Netherlands, 2000.

Table 2. Crystal Data for (p-tBuBz)$_2$Ca·(THF)$_4$, (Bz)$_2$Ca·(THF)$_4$, and [Ph$_3$C$^-$]$_2$[Ca^{2+}·(THF)$_6$]

	(p-tBuBz)$_2$Ca·(THF)$_4$	(Bz)$_2$Ca·(THF)$_4$	[Ph$_3$C$^-$]$_2$[Ca^{2+}·(THF)$_6$]
formula	$C_{38}H_{62}CaO_4$	$[C_{30}H_{46}CaO_4]_2[C_6H_6]$	$[C_{19}H_{15}]_2[C_{24}H_{48}CaO_6]$
MW	622.96	1099.56	959.33
size (mm^3)	0.3 × 0.3 × 0.7	0.3 × 0.4 × 0.5	0.2 × 0.2 × 0.2
cryst syst	triclinic	triclinic	cubic
space group	$P\bar{1}$	$P\bar{1}$	F_d-3
a (Å)	7.759(2)	8.726(1)	28.265(4)
b (Å)	14.131(3)	16.545(5)	28.265(4)
c (Å)	17.141(3)	22.560(8)	28.265(4)
α (deg)	92.47(1)	75.94(2)	90
β (deg)	91.52(2)	81.61(1)	90
γ (deg)	91.89(2)	89.90(3)	90
V (Å^3)	1875.9(7)	3123.8(15)	22581(6)
Z	2	2	16
ρ (g cm^{-3})	1.103	1.169	1.129
μ(Mo Kα) (mm^{-1})	0.202	0.234	0.159
T (°C)	−90	−120	−120
θ(max)	25.5	26.0	25.0
no. of unique reflns	6951	12 289	1674
no. of obsvd reflns ($I > 2\sigma(I)$)	5266	5820	701
no. of params	537	844	157
R_1	0.059	0.069	0.056
wR_2	0.172	0.189	0.175
GOF	1.04	1.02	1.00
max./min. resd (e Å^{-3})	−0.47/0.44	−0.46/0.52	−0.45/0.61

used in the discussion of the C−H···aryl interactions. The use of calculated positions with realistic C−H distances is closer to reality, is more accurate, and allows a better comparison of the results.[5]

Ab initio calculations (MP2/6-31+G*) of the free anions were performed with the computer program Gaussian 98.[14] All optimized structures (C_s-symmetry) are true minima. DFT calculations (BP86/lacvp*+) were performed without symmetry restrictions using the program Jaguar.[15]

Synthesis of *p*-*t*Bu-benzylpotassium. *n*-Butyllithium (1.6 M, 16.0 mL, 25.0 mmol) was added dropwise to a solution of *p*-*t*Bu-toluene (5.00 g, 33.7 mmol) in THF (25 mL) and potassium 3-methyl-3-pentanolate (4.10 g, 29.0 mmol) precooled at −70 °C (the BuLi was added such that drops float along the cooled walls of the Schlenk tube). The solution was stirred at this temperature for ca. 1−2 h and turned red. Subsequently, the solution was slowly warmed to 0 °C, and the solvents were removed under vacuum, allowing the temperature to rise to 20 °C in the later stages. The orange solid was washed five times with 40 mL portions of hexane. Drying the product under vacuum (25 °C, 1 Torr, 30 min) resulted in an orange powder (quantitative yield: 4.80 g). ^{1}H NMR (C_6D_6/THF-d_8, 250 MHz, 20 °C): 1.26 (s, 9H, *t*Bu); 2.41 (s, 2H, CH$_2$); 5.88 (d, 8.5 Hz, 2H, aryl); 6.49 (d, 8.5 Hz, 2H, aryl). ^{13}C NMR (C_6D_6/THF-d_8, 250 MHz, 20 °C): 32.2 (Me); 33.1 (C$_q$); 48.3 (CH$_2$); 109.9 (C$_{ortho}$); 118.9 (C$_{para}$); 127.5 (C$_{meta}$); 151.3 (C$_{ipso}$).

Synthesis of *p*-Me$_3$Si-benzylpotassium. *n*-Butyllithium (2.6 M, 7.8 mL, 20.0 mmol) was added dropwise to a solution of *p*-Me$_3$Si-toluene (4.00 g, 24.4 mmol) in THF (20 mL) and potassium 3-methyl-3-pentanolate (3.08 g, 22.0 mmol) precooled at −70 °C (the BuLi was added such that drops float along the cooled walls of the Schlenk tube). The solution was stirred at this temperature for ca. 1−2 h and slowly turned red. Subsequently, the solution was slowly warmed to 0 °C, and the solvents were removed under vacuum, allowing the temperature to rise to 20 °C in the later stages. The orange solid was washed five times with 40 mL portions of hexane. Drying the product under vacuum (25 °C, 1 Torr, 30 min) resulted in an orange powder (3.70 g, 18.3 mmol, 92%). ^{1}H NMR (C_6D_6/THF-d_8, 250 MHz, 20 °C): 0.20 (s, 9H, Me$_3$Si); 2.81 (s, 2H, CH$_2$); 5.91 (d, 8.4 Hz, 2H, aryl); 6.55 (d, 8.4 Hz, 2H, aryl). ^{13}C NMR (C_6D_6/THF-d_8, 250 MHz, 20 °C): 0.3 (Me$_3$Si); 57.8 (CH$_2$); 98.7 (C$_{para}$); 111.2 (C$_{ortho}$); 135.8 (C$_{meta}$); 151.2 (C$_{ispo}$).

Synthesis of Bis[*p*-*t*Bu-benzyl]calcium·(THF)$_4$. Addition of CaI$_2$ (4.00 g, 13.6 mmol) to a solution of *p*-*t*Bu-benzylpotassium (4.98 g, 26.7 mmol) in 60 mL of THF resulted in a gradual color change of red to orange. The suspension was stirred for 24 h, and the solvent was removed under vacuum. The product was extracted from the residue with two 50 mL portions of benzene. The solvent of the combined benzene extracts was removed under vacuum, and the resulting orange foam was recrystallized by cooling a THF/hexane (1/1) solution to −20 °C. The product crystallizes in the form of yellow needles (3.40 g, 5.47 mmol, 41%). $C_{38}H_{62}O_4Ca$ (calcd C 73.27 and H 10.03, found C 72.81 and H 9.78). ^{1}H NMR (C_6D_6/THF-d_8, 250 MHz, 20 °C): 1.37 (s, 18H, *t*Bu); 1.41 (m, 16H, THF); 1.77 (s, 4H, CH$_2$); 3.55 (m, 16H, THF); 6.67 (d, 8.4 Hz, 4H, aryl); 6.98 (d, 8.4 Hz, 4H, aryl). ^{13}C NMR (C_6D_6/THF-d_8, 250 MHz, 20 °C): 25.7 (THF); 32.3 (Me); 33.6 (C$_q$); 39.9 (CH$_2$); 68.0 (THF); 119.0 (C$_{ortho}$); 125.2 (C$_{meta}$); 131.6 (C$_{para}$); 157.3 (C$_{ipso}$).

Synthesis of Bis[*p*-Me$_3$Si-benzyl]calcium·(THF)$_4$. Addition of CaI$_2$ (2.97 g, 10.1 mmol) to a solution of *p*-Me$_3$Si-benzylpotassium (4.08 g, 20.2 mmol) in 35 mL of THF resulted in a gradual color change of red to orange. The suspension was stirred for 24 h, and the solvent was removed under vacuum. The product was extracted from the residue with two 40 mL portions of benzene. The solvent of the combined benzene extracts was removed under vacuum, and the resulting orange powder was recrystallized by cooling a THF/hexane (1/1) solution to −20 °C. The product crystallizes in the form of very thin yellow needles unsuitable for X-ray diffraction (3.90 g, 5.96 mmol, 59%). ^{1}H NMR (C_6D_6/THF-d_8, 250 MHz, 20 °C): 0.28 (s, 18H, Me$_3$Si); 1.44 (m, 16H, THF); 1.88 (s, 4H, CH$_2$); 3.54 (m, 16H, THF); 6.61 (d, 8.4 Hz, 4H, aryl); 7.06 (d, 8.4 Hz, 4H, aryl). ^{13}C NMR (C_6D_6/THF-d_8, 250 MHz, 20 °C): 0.0 (Me$_3$Si); 25.7 (THF); 44.0 (CH$_2$); 67.6 (THF); 115.0 (C$_{para}$); 118.7 (C$_{ortho}$); 134.1 (C$_{meta}$); 160.3 (C$_{ipso}$).

---

(14) M. J. Frisch, G. W. Trucks, H. B. Schlegel, G. E. Scuseria, M. A. Robb, J. R. Cheeseman, V. G. Zakrzewski, J. A. Montgomery, Jr., R. E. Stratmann, J. C. Burant, S. Dapprich, J. M. Millam, A. D. Daniels, K. N. Kudin, M. C. Strain, O. Farkas, J. Tomasi, V. Barone, M. Cossi, R. Cammi, B. Mennucci, C. Pomelli, C. Adamo, S. Clifford, J. Ochterski, G. A. Petersson, P. Y. Ayala, Q. Cui, K. Morokuma, D. K. Malick, A. D. Rabuck, K. Raghavachari, J. B. Foresman, J. Cioslowski, J. V. Ortiz, A. G. Baboul, B. B. Stefanov, G. Liu, A. Liashenko, P. Piskorz, I. Komaromi, R. Gomperts, R. L. Martin, D. J. Fox, T. Keith, M. A. Al-Laham, C. Y. Peng, A. Nanayakkara, C. Gonzalez, M. Challacombe, P. M. W. Gill, B. G. Johnson, W. Chen, M. W. Wong, J. L. Andres, M. Head-Gordon, E. S. Replogle, J. A. Pople. *Gaussian 98* (Revision A.7); Gaussian, Inc.: Pittsburgh, PA, 1998.

(15) *Jaguar 5.0*; Schrödinger, LLC: Portland, Oregon, 2002.

Synthesis of Bis[benzyl]calcium·(THF)$_4$. Addition of CaI_2 (10.5 g, 35.7 mmol) to a solution of benzylpotassium (10.0 g, 77.0 mmol) in 150 mL of THF resulted in a slight temperature rise and a gradual color change of red to orange. The suspension was stirred for 24 h and was centrifugated. The mother liquor was separated, and the THF solvent was removed under vacuum (resulting in a red viscous oil). The residue of centrifugation was extracted twice with 100 mL portions of benzene. Both benzene extracts were added to the red viscous oily product, and the solution was concentrated to a volume of ca. 125 mL. Cooling to +5 °C resulted in the formation of large yellow crystals (11.05 g; 21.5 mmol, 60%). ^{1}H NMR (C_6D_6/THF-d_8, 250 MHz, 20 °C): 1.44 (m, 16H, THF); 1.80 (s, 4H, CH_2); 3.54 (m, 16H, THF); 6.29 (t, 7.1 Hz, 2H, aryl); 6.68 (d, 7.3 Hz, 4H, aryl); 6.97 (t, 7.2 Hz, 4H, aryl). ^{13}C NMR (C_6D_6/THF-d_8, 250 MHz, 20 °C): 25.7 (THF); 41.6 (CH_2); 68.0 (THF); 109.6 (C_{para}); 119.2 (C_{ortho}); 128.6 (C_{meta}); 160.2 (C_{ipso}).

Synthesis of [Ph$_3$C$^-$]$_2$ [Ca^{2+}·(THF)$_4$]. Addition of (2.58 g, 10.6 mmol) of Ph_3CH to an orange-red solution of bis[benzyl]-calcium·(THF)$_4$ (2.70 g, 5.29 mmol) in 20 mL of benzene and 2 mL of THF resulted in an immediate change of color to dark red. The solution was stirred for 2 h at 70 °C, after which the solvents were removed under vacuum. The resulting red foam was washed with 10 mL of hexane and dissolved in 20 mL of benzene. Slow vapor diffusion of THF gives dark red crystals with a green-metallic shine in the form of octahedrons (4.82 g, 5.02 mmol, 95%). $C_{62}H_{78}O_6Ca$ (calcd C 77.63 and H 8.20, found C 77.40 and H 8.11). ^{1}H NMR (C_6D_6/THF-d_8, 250 MHz, 20 °C): 1.32 (m, 24H, THF); 3.45 (m, 24H, THF); 6.41 (t, 7.0 Hz, 6H, aryl); 6.87 (t, 7.8 Hz, 12H, aryl), 7.28 (d, 8.0 Hz, 12H, aryl). ^{13}C NMR (C_6D_6/THF-d_8, 250 MHz, 20 °C): 25.7 (THF); 68.5 (THF); 90.3 (C_α); 116.3 (C_{para}); 123.0 (C_{ortho}); 129.9 (C_{meta}); 146.1 (C_{ipso}).

Acknowledgment. We are grateful to the Deutsche Forschungsgemeinschaft and the BASF AG (Ludwigshafen, Germany) for financing this project. Dr. M. Ringwald (MCAT, Konstanz, Germany) is kindly acknowledged for large amounts of benzylpotassium.

Supporting Information Available: All crystallographic information for the crystal structures (bond distances and angles, crystal data, refinement details, ORTEP plots) is available free of charge via the Internet at http://pubs.acs.org.

OM0341350